

than 100  $\mu\text{m}$ . Such short distances might mark the lower limit of the suggested method for photolithographic patterning.

The observed effect of degradation in the dark suggests that dark pores in titanium dioxide particles may have large effect on the photocatalytic performance. As the separation cost of small, highly photoactive titanium dioxide particles, such as the Degussa P-25, is quite high, these results suggest that it may be worth developing relatively large, yet highly porous, titanium dioxide particles, even if these pores are shielded from the impinging UV light.

*This work was funded by the Israeli Ministry of Science, and by the 5th framework of the European Commission (INCOMED).*

- [1] A. Fujishima, K. Hashimoto, T. Watanabe, *TiO<sub>2</sub> Photocatalysis: Fundamentals and Applications*, BKC, Tokyo, 1996.
- [2] P. Salvador, *J. Electrochem. Soc.* **1981**, *128*, 1895–1900.
- [3] V. A. Henrich, D. Dresselhaus, H. J. Zeiger, *Phys. Rev. Lett.* **1976**, *36*, 158–161.
- [4] A. Fujishima, T. N. Rao, D. A. Tryk, *J. Photochem. Photobiol. C: Photochem. Rev.* **2000**, *1*, 1–21.
- [5] a) L. Sopyan, M. Watanabe, S. Murasawa, K. Hashimoto, A. Fujishima, *J. Photochem. Photobiol. A: Chem.* **1996**, *98*, 79–86; b) J. Peral, D. F. Ollis, *J. Catal.* **1992**, *136*, 554–565.
- [6] a) M. Muneer, S. Das, V. B. Manilal, A. Haridas, *J. Photochem. Photobiol. A: Chem.* **1992**, *63*, 107–114; b) R. W. Matthews, *J. Phys. Chem.* **1987**, *91*, 3328–3333.
- [7] Y. Kikuchi, K. Sunada, T. Iyoda, K. Hashimoto, A. Fujishima, *J. Photochem. Photobiol. A: Chem.* **1997**, *106*, 51–56.
- [8] S. Kim, W. Choi, *Environ. Sci. Technol.* **2002**, *36*, 2019–2025.
- [9] T. Tatsuma, S. I. Tachibana, T. Miwa, D. Tryk, A. Fujishima, *J. Phys. Chem. B* **1999**, *103*, 8033–8035.
- [10] T. Tatsuma, S. I. Tachibana, A. Fujishima, *J. Phys. Chem. B* **2001**, *105*, 6987–6992.
- [11] H. Haick, Y. Paz, *J. Phys. Chem. B* **2001**, *105*, 3045–3051.
- [12] E. Zemel, H. Haick, Y. Paz, *J. Adv. Oxid. Technol.* **2002**, *5*(1), 27–32.
- [13] C. L. Lee, W. Choi, *J. Phys. Chem. B* **2002**, *106*, 11 818–11 822.
- [14] a) M. Zayats, M. Lahav, A. B. Kharitonov, I. Willner, *Tetrahedron* **2002**, *58*(4), 815–824; b) A. Suzuki, M. Tada, T. Sasaki, T. Shido, Y. Iwasawa, *J. Mol. Catal. A: Chem.* **2002**, *182–183*, 125–136; c) S. W. Lee, I. Ichinose, T. Kunitake, *Langmuir* **1998**, *14*(10), 2857–2863.
- [15] J. Schwitzgebel, J. G. Ekerdt, H. Gerischer, A. Heller, *J. Phys. Chem.* **1995**, *99*, 5633–5638.
- [16] K. I. Ishibashi, Y. Nosaka, K. Hashimoto, A. Fujishima, *J. Phys. Chem. B* **1998**, *102*, 2117–2120.
- [17] P. Sawunyama, A. Fujishima, K. Hashimoto, *Langmuir* **1999**, *15*, 3551–3556.
- [18] Y. Ohko, K. Hashimoto, A. Fujishima, *J. Phys. Chem. A* **1997**, *101*, 8057–8062.
- [19] N. Takeda, M. Ohtani, T. Torimoto, S. Kuwabata, H. Yoneyama, *J. Phys. Chem. B* **1997**, *101*, 2644–2649.
- [20] Y. Paz, Z. Luo, L. Rabenberg, A. Heller, *J. Mater. Res.* **1995**, *10*, 2842–2848.
- [21] A. N. Parikh, D. L. Allara, I. B. Azouz, F. Rondelez, *J. Phys. Chem.* **1994**, *98*, 7577–7590.
- [22] H. Gerischer, A. Heller, *J. Phys. Chem.* **1991**, *95*, 5261–5267.
- [23] R. Memming, *Top. Curr. Chem.* **1994**, *169*, 105–181.
- [24] A. Dawson, P. Kamat, *J. Phys. Chem. B* **2001**, *105*, 960–966.
- [25] G. R. Bamwenda, S. Tsubota, T. Nakamura, M. Haruta, *J. Photochem. Photobiol. A: Chem.* **1995**, *89*, 177–189.
- [26] D. E. Eastman, *Phys. Rev. B* **1970**, *3*, 1–2.
- [27] R. C. Reid, T. K. Sherwood, *The Properties of Gases and Liquids*, McGraw-Hill, NY, **1958**, Chap. 8.
- [28] J. G. Szezechowski, C. A. Koval, R. D. Noble, *J. Photochem. Photobiol. A: Chem.* **1993**, *74*, 273–278.
- [29] T. Tatsuma, W. Kubo, A. Fujishima, *Langmuir* **2002**, *18*, 9632–9634.

Received: December 19, 2002 [Z622]

## Mechanism of Lck Recruitment to the T-Cell Receptor Cluster as Studied by Single-Molecule-Fluorescence Video Imaging

Hiroshi Ike,<sup>[a]</sup> Atsushi Kosugi,<sup>[b]</sup> Akiko Kato,<sup>[b]</sup> Ryota Iino,<sup>[a]</sup> Hidemi Hirano,<sup>[a]</sup> Takahiro Fujiwara,<sup>[a]</sup> Ken Ritchie,<sup>[a, c]</sup> and Akihiro Kusumi<sup>\*,[a, c]</sup>

### KEYWORDS:

membranes · Lck · signal transduction · single-molecule studies

### Introduction

The T-cell receptor (TCR) signaling has fascinated many researchers, because, in addition to its immunological importance, it appears to provide interesting paradigms for the study of the basic design/concepts on how cellular signaling transduction is carried out and regulated. The multiple signaling pathways triggered by TCR involve various conceptually different and important mechanisms for the regulation of simultaneously working signaling;<sup>[1, 2]</sup> some signaling pathways have to be activated continuously for a long time (over 24 h);<sup>[3]</sup> the TCR signaling network should contain circuits to prevent and/or turn off faulty signals;<sup>[4]</sup> and it should amplify or reduce the signal when another signal comes from coreceptors, such as CD28 and CD4/8.<sup>[5]</sup> T cells achieve such complex signal transduction by recruiting specific signaling molecules to the TCR clusters and their neighborhood, and also by having them escape from the stimulation zone, in the correct order and at the right time;<sup>[6]</sup> in other words, the recruitment process itself is the fundamental regulation mechanism for this complex signal transduction.

Herein, we study the regulation mechanism by which Lck, a Src family kinase, is recruited to the site of TCR clustering. Lck is recruited to the site of TCR clustering during the very early stages after TCR engagement.<sup>[7]</sup> We observed single molecules of Lck and its N-terminal ten amino acid sequence (N10), both fused with green fluorescent protein (GFP) (Lck- and N10-GFP, respectively, Figure 1A) and expressed in the Jurkat T cell line,

[a] A. Kusumi, H. Ike, R. Iino, H. Hirano, T. Fujiwara, K. Ritchie  
Kusumi Membrane Organizer Project  
Exploratory Research for Advancement of Technology Organization (ERATO), JST, Nagoya, 460-0012 (Japan)  
Fax: (+81) 52-789-2968  
E-mail: akusumi@bio.nagoya-u.ac.jp

[b] A. Kosugi, A. Kato  
School of Allied Health Sciences  
Faculty of Medicine  
Osaka University, Toyonaka, 565-0871 (Japan)

[c] A. Kusumi, K. Ritchie  
Department of Biological Science and Institute for Advanced Research  
Nagoya University  
Nagoya, 464-8602 (Japan)

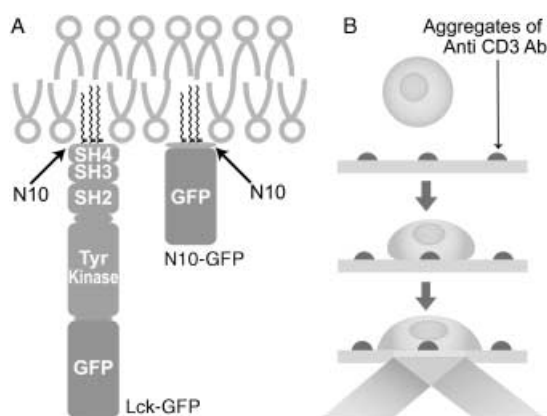


**Figure 1.** Molecular structures of Lck- and N10-GFP, and the experimental protocol for the local stimulation and the subsequent observation of the Jurkat cells employed here. A) Lck has three saturated fatty acyl (one myristoyl and two palmitoyl) chains at its N-terminal ten amino acid region (N10). Through these saturated acyl chains, Lck and N10 bind to the inner leaflet of the plasma membrane, and partition into the detergent-resistant membrane (DRM) fraction (about 50% of Lck and 80% of N10). The N10 domain is included in the SH4 domain, which also includes the CD4 binding site. After the SH4 domain are an SH3 domain and SH2 domain, which interact with other proteins, and finally the tyrosine kinase domain at the C-terminus of the full-length Lck kinase. To visualize these molecules, we used N10 fused to GFP (N10-GFP) and the full-length Lck fused to GFP (Lck-GFP). B) The experimental protocol employed here to induce TCR clustering and triggering of the downstream signaling events from a single localized spot in a cell. Aggregates of anti-CD3 $\epsilon$  (a subunit of the TCR complex) antibody (OKT3) were sparsely adsorbed onto cover slips. The cells were lightly centrifuged onto the cover slip, and the cells that landed on aggregates of anti-CD3 antibody (an aggregate per cell) were used for further experiments. TIRF microscopy was performed to observe the Lck- and N10-GFP molecules on the cell membrane facing the cover slip.

using single fluorophore video imaging.<sup>[8, 9]</sup> Lck consists of an SH4 domain which includes the N10 and the domain for the interaction with a coreceptor CD4, an SH3 domain, an SH2 domain, and a kinase domain. N10 has no site for specific interactions with other proteins, but contains all of the Lck anchoring, saturated alkyl chains (one myristoyl and two palmitoyl), which induce the partitioning of about half of Lck<sup>[10]</sup> and 80% of N10-GFP (this study, data not shown) into the detergent-resistant membrane (DRM) fraction.

Two mechanisms have been proposed for Lck recruitment: one is that Lck is carried along with its binding protein, CD4, which is recruited to the TCR clustering site due to its affinity to MHC II in the antigen-presenting cell (the target cell; MHC II binds to both TCR and CD4);<sup>[11]</sup> and the other is that the Lck molecules associated with the raft are assembled when the rafts are carried by the actomyosin system to the site of TCR clustering.<sup>[12]</sup>

Since we are concerned with events occurring at the very early stages of TCR signaling, a simplified model system has been developed in this research. First, the TCR clustering was induced at a single site in a cell using aggregates of OKT3, an antibody against CD3 $\epsilon$ , one of the subunits of the TCR complex, and the cell was very locally stimulated. The antibody aggregate induced TCR clustering, which in turn triggered the subsequent cellular signaling, including Lck assembly. In other words, with the aggregates of the anti-CD3 $\epsilon$  antibody, we tried to mimic antigen

presentation to the T cell by locally inducing TCR clustering. To do this, aggregates of OKT3 were sparsely adsorbed on a cover slip, and then the cells were centrifuged onto it. By quickly sedimenting the cells onto the cover slip, the initial time for TCR clustering is defined. Bunnell et al.<sup>[13]</sup> previously coated the cover slip with an anti-CD3 $\epsilon$  antibody to induce cellular signaling from all over the surface of cells attached to the cover slip, and the cell was extensively extended on the cover slip. In the present strategy, by using the antibody aggregates, we carried out very local stimulation at a single, small site per cell.

Second, to investigate the Lck recruiting process, we expressed Lck- and N10-GFP fusions in Jurkat cells. For the investigation of the initial signaling processes, the Jurkat cells could mimic the primary T cells *in vivo* and provide a simpler experimental cell system for transfection with these cDNAs.

Third, individual molecules of Lck- and N10-GFP were observed by single-fluorescent-molecule video imaging, using an objective-lens type total internal reflection fluorescence (TIRF) microscopy. By observing the behavior of single molecules at video rate, the local events occurring after stimulation can be investigated at the spatial resolution of single molecules.

## Materials and Methods

### Plasmid Constructs

The DNA fragment encoding the full-length Lck was obtained from the vector described previously<sup>[14]</sup> by NotI digestion, followed by the treatment with Klenow fragment and dNTP and then digestion with XhoI. Excised fragments were ligated into the pEGFP expressing vector (Clontech) that had been digested with SmaI and XhoI (Lck-GFP). For the vector expressing the first 10 amino acids of Lck fused to GFP (N10-GFP), an oligolinker encoding the first ten amino acids of Lck was inserted into the Xho/SalI sites of LAT(TM)-FLAG-GFP in pMKIT Neo, and the SR $\alpha$  promoter-driven expression vector, by replacing the LAT(TM) portion with the N-terminal part of Lck. The LAT(TM)-FLAG-GFP was constructed from the LAT(TM)-FLAG-SHP-1, by replacing the SHP-1 portion with EGFP.<sup>[15]</sup> The vector for GFP-actin was described previously.<sup>[16]</sup>

### Cell Culture

Jurkat cells were grown in RPMI1640 medium supplemented with 10% fetal bovine serum (FBS). These cells were transfected using either a Gene Pulser II (BioRad) or DMRIE-C (Invitrogen), according to the manufacturers' recommendations. For the observation of N10-GFP, cells stably expressing this molecule were used. For the experiments observing Lck-GFP and actin-GFP, cells transiently expressing these molecules were used.

### Local Stimulation of Jurkat Cells

Aggregates of the mouse monoclonal antibody OKT3, directed against a subunit of the TCR complex, CD3 $\epsilon$ , were formed by mixing rat antigoat IgG (Oriental Yeast, 1  $\mu$ L of 1 mg mL<sup>-1</sup>), goat antistreptavidin (Biomedica, 2  $\mu$ L of 1 mg mL<sup>-1</sup>), streptavidin

(Sigma, 4  $\mu\text{L}$  of 1  $\text{mg mL}^{-1}$  containing 10% Alexa594-labeled streptavidin), biotinylated rat antimouse IgG (Molecular Probes, 8  $\mu\text{L}$  of 2  $\text{mg mL}^{-1}$ ), and OKT3 (hybridoma obtained from ATCC, 32  $\mu\text{L}$  of 1  $\text{mg mL}^{-1}$ ), in this order. Free antibodies, streptavidin, and small aggregates in the suspension were removed by three cycles of centrifugation (16,000  $\times g$  for 15 min) and resuspension, and finally the pellet of the aggregated antibodies was resuspended in 0.2 mL of phosphate-buffered saline (PBS). The suspension containing only large aggregates was placed on the cover slip (12 mm  $\phi$ ) of the glass-base dish (Iwaki), incubated for 3 min, and washed with PBS twice. The cover slip was then coated with poly-L-lysine by an incubation in a 1  $\mu\text{g mL}^{-1}$  poly-L-lysine solution for 1 min. The Jurkat cells were centrifuged onto the cover slip at 850  $\times g$  for 1 min, and were immediately used for microscopy. Only those cells that landed onto an aggregate of OKT3 in their central regions were used for further observations.

### Imaging and Analysis

Single GFP fusion proteins expressed in Jurkat cells were observed by using an objective-lens type TIRF microscope, as described previously.<sup>[8, 9, 17]</sup> The trajectories of the fluorescent molecules were obtained from video images, and were analyzed as described previously.<sup>[8, 17–19]</sup>

### Drug treatment

Jurkat cells were pretreated with 4 mM methyl- $\beta$ -cyclodextrin (M $\beta$ CD)(Wako)<sup>[10]</sup> or 10  $\mu\text{M}$  cytochalasin D (Sigma)<sup>[20]</sup> for 15 min before attachment to the cover slip for observation. These drug concentrations were maintained throughout the experiment (approximately 10 min).

## Result and Discussion

### Local Stimulation of a Jurkat Cell by a Single Aggregate of the Anti-TCR Antibody

To define the space–time of stimulation in the Jurkat cell clearly, a method was developed to stimulate the cell at a single site. Large aggregates of the anti-CD3 $\epsilon$  antibody were generated, as described in the Materials and Methods section, and were sparsely adsorbed onto a cover slip (which was then coated with poly-L-lysine). The Jurkat cells (which do not adhere to the glass surface) were centrifuged onto the sparsely distributed aggregates of anti-CD3 $\epsilon$  antibody on the cover slip, and those that landed on a single cluster in the central region of the cell were examined (Figure 1 B). It took about 4 min from the start of the centrifugation until the initiation of the TIRF microscopic observation (1.5 min for centrifugation, 0.5 min for transfer to the microscope stage, and 2 min to find a cell to be observed). The plasma membrane located adjacent to the cover slip was inspected (generally a circular area of  $\approx 5 \mu\text{m}$  in radius).

Jurkat cells were locally stimulated by these aggregates of anti-CD3 $\epsilon$  antibody (single stimulation point per cell). The idea was that these aggregates would induce the TCR clusters on the

Jurkat cell surface, which would subsequently trigger the downstream signaling pathways. Right after the microscopic observation was initiated (4 min after the cell sedimentation by centrifugation was started), we found that the TCR had already become clustered on top of the antibody aggregates, and that the  $\text{Ca}^{2+}$  ion level in the cytoplasm (as observed with a fluorescent calcium indicator dye fluo4) had already become elevated, as compared with the TCR aggregation and the  $\text{Ca}^{2+}$  ion levels in nearby cells that did not land on the antibody aggregates (data not shown). These results suggest that a single antibody aggregate is sufficient to stimulate the Jurkat cell.

### Assembly of Lck- and N10-GFP at the Site of TCR Clustering (Stimulation Point)

Figure 2 shows the distributions of Lck- and N10-GFP, with and without local stimulation with the antibody aggregate. The distribution of Lck-GFP (and N10-GFP) on the plasma membranes of unstimulated cells was mostly homogeneous. However, in a cell that landed on an antibody aggregate, both Lck- and N10-GFP were concentrated at and around the stimulation-

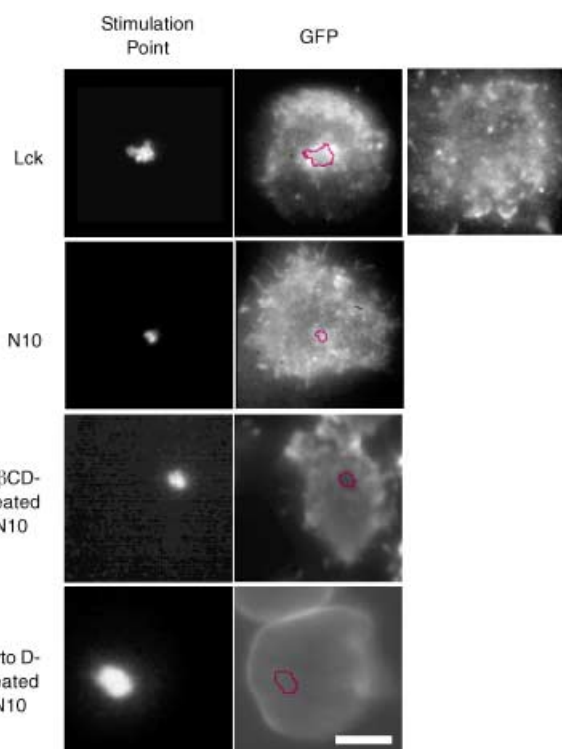


**Figure 2.** Recruitment of Lck- and N10-GFP to the stimulation point. Fluorescent images of the antibody aggregates (streptavidin labeled with Alexa594) are shown on the left, and their contours are shown in magenta lines in the Lck- and N10-GFP images on the right. Both Lck-GFP and N10-GFP are concentrated not only at the stimulation point but also in the area surrounding the point. The Lck image on the right shows the cell that did not land on the antibody aggregate. After mild treatments with 4 mM M $\beta$ CD or 10  $\mu\text{M}$  cytochalasin D for 15 min, the assembly of these molecules was blocked. Bar: 3  $\mu\text{m}$ .

point, although the majority of these molecules were still distributed over the cell surface. This occurred quickly, because such assembly was observed even at the initiation of the observation.

However, the fluorescent intensities at and near the stimulation point did not increase considerably after the initial observation at  $\approx 4$  min after centrifugation (up to 20 min after centrifugation, our longest observation point). Meanwhile, the recruitment of Lck- and N10-GFP continued during this observation period, since even after the assembled molecules were photobleached, the fluorescent intensity at and around the stimulation point recovered in less than a minute (data not shown). These results indicate that the Lck- and N10-GFP molecules are continuously being recruited to the region of stimulation as well as migrating away from the neighborhood of the stimulation point after their recruitment.

The localization of N10-GFP at and near the stimulation point indicates that Lck does not require interactions in the protein moiety for its recruitment to the TCR cluster, that is, Lck binding to CD4 is not crucial for Lck recruitment to the stimulation point. This suggests that the association of N10-GFP with rafts via the three saturated acyl chains may be sufficient for localizing N10 and Lck to the TCR cluster. However, the Lck association with CD4, via Lck's SH4 domain, may also play a role in the recruitment of Lck or the elongation of its residency time near the stimulation point.

The concentration of Lck- and N10-GFP at the stimulation point was inhibited by a treatment with either M $\beta$ CD or cytochalasin D (see Figure 2). These results suggest that the recruitment of Lck requires both rafts and intact actin filaments. These observations are consistent with the previously proposed model by Moran and Miceli,<sup>[12]</sup> in which the signaling molecules associated with rafts are assembled to the stimulation point by directed transport by the actomyosin system (although the models diverge here, as described later). In addition, the relationship between the Lck recruitment and the actin filament assembly/reorganization may be complicated. For the initial signaling for actin reorganization, a small Lck signal (perhaps induced by the diffusional collision and entrapment of Lck by the TCR cluster, and the triggering of the SLP-76 pathway at a low level) may be required. The reorganized actin filaments may recruit Lck more efficiently, which would further concentrate the actin filaments near the stimulation point. This concentration may in turn cause a large-scale, long-lasting concentration of Lck at the stimulation point. The initial reorganization of the actin filaments may also be induced by the binding of the actin filaments to the  $\zeta$  chains of the TCR cluster.<sup>[21]</sup> Rafts may also be required for temporarily keeping Lck on the TCR cluster; Lck may partition into the raft stabilized by clustering of TCR or the raft Lck is associated with may coalesce with the TCR-cluster rafts.

### Single-Molecule Dynamics of Lck-GFP and N10-GFP After Point Stimulation

To investigate the localization mechanism of Lck- and N10-GFP, the motions of these molecules expressed in Jurkat cells were observed at the level of single molecules, by using TIRF

microscopy in the plasma membrane facing the cover slip (Figure 3A). These spots exhibited single-step photobleaching (Figure 3B) and a Gaussian-like intensity profile of a single peak (Figure 3C), which indicates that single molecules of Lck- and

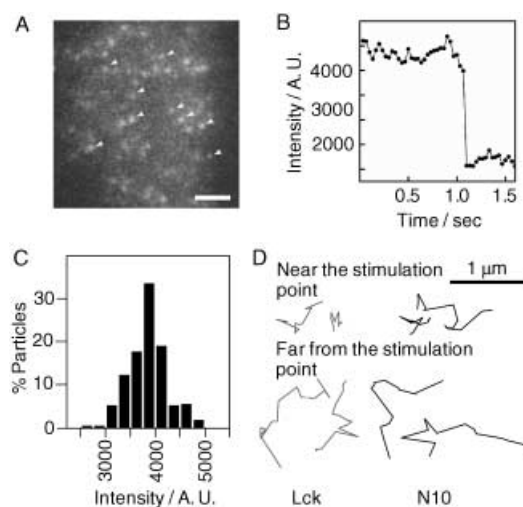


**Figure 3.** Single-fluorophore video imaging of Lck- and N10-GFP. A) A snapshot of a video-image sequence, showing single Lck-GFP molecules (arrowheads) expressed in Jurkat cells. Bar: 3  $\mu$ m. B) A typical example of the single-step photobleaching of an Lck-GFP spot, observed at video rate. C) Distribution of the fluorescence intensity of individual Lck-GFP spots. D) Typical trajectories of Lck- and N10-GFP spots located near and far from the stimulation point and without local stimulation.

N10-GFP can be imaged in the plasma membrane. Since the fluorescence intensities of the Lck- and N10-GFP spots, as well as those of the spots of fluorescein laurate incorporated in the membrane, exhibited single-peak, Gaussian-like distributions, we concluded that the membrane regions closely facing the cover slip are almost flat.

Representative trajectories of single molecules of Lck- and N10-GFP are shown in Figure 3D. Since GFP photobleaches rapidly, with a lifetime of 0.5 s under the present experimental conditions, only short trajectories could be obtained. The molecules apparently undergo simple Brownian diffusion in this short time window. The average diffusion coefficients determined in the time window of 100 ms (D100 ms) are plotted against the distance from the stimulation point (Figure 4). For comparison, D100 ms without stimulation is also shown. The D100 ms values for Lck- and N10-GFP were both lower near the local stimulation point, as compared to those from that without stimulation, whereas they were higher in the areas far from the stimulation point.

As described above, both the Lck- and N10-GFP molecules appeared to be recruited and then to move away. However, due to the short GFP lifetime, we were unable to trace the same molecule approaching and leaving the stimulation point.

After treatments with M $\beta$ CD or cytochalasin D, the movements of Lck- and N10-GFP became very fast, even in locally stimulated cells (the movement was fast everywhere). The D100 ms was over 5  $\mu$ m<sup>2</sup>s<sup>-1</sup>, which prevented us from making

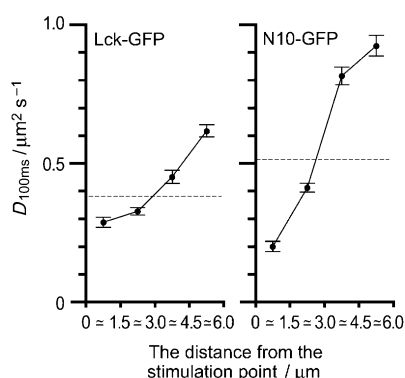


**Figure 4.** The average diffusion coefficients (in a 100 ms window) for Lck-GFP and N10-GFP were lower near the local stimulation point, whereas they were higher in the areas far from the stimulation point. The diffusion coefficient ( $D_{100\text{ ms}}$ ) is plotted as a function of the distance between the first point of the trajectory and the center of gravity of the stimulation point (averaged in the following regions: 0–1.5, 1.5–3.0, 3.0–4.5, and greater than 4.5  $\mu\text{m}$ ). The  $D_{100\text{ ms}}$  value in the cells without stimulation is shown by the broken line in each figure.

precise measurements of  $D_{100\text{ ms}}$  under these conditions. However, these results indicate that the rafts and the actin membrane skeleton (cortical actin filaments) together play major roles in suppressing the diffusion of Lck- and N10-GFP.

These results can be understood by the corralling (membrane skeleton fence model) and tethering effects of the membrane skeleton,<sup>[22]</sup> as well as by the corralling effects of various transmembrane picket proteins anchored to the actin membrane skeleton (picket model<sup>[17]</sup>). Many membrane-associated proteins have cytoplasmic domains, and in the membrane skeleton fence model, these cytoplasmic domains collide with the actin-based membrane skeleton closely apposed to the cytoplasmic surface of the plasma membrane, which induces the temporal confinement of these proteins in the meshwork of the membrane skeleton. These proteins may also be tethered or anchored to the membrane skeleton, which would also suppress their diffusion. In the latter, the picket model,<sup>[17]</sup> the various transmembrane proteins anchored to the membrane skeleton (even for a short period of time, if it is longer than the characteristic time for the membrane molecules to pass the boundary region between the compartments, which may be on the order of a microsecond or less) effectively act as rows of pickets against the free diffusion of lipids, proteins, and any other molecules dissolved in the membrane, due to the steric hindrance and hydrodynamic frictionlike effects of the immobile proteins anchored to the membrane skeleton.

Based on these previous observations, we propose that the movement of the monomeric forms of the Lck- and N10-GFP molecules will be suppressed by the corralling and tethering effects of the membrane skeleton,<sup>[22]</sup> as well as by the corralling effects of the various transmembrane picket proteins anchored to the actin membrane skeleton.<sup>[17]</sup> Furthermore, we envisage that when these proteins are localized in the stable rafts containing many molecules, the corralling and tethering effects of the picket-fence on the Lck- and N10-GFP molecules would be greatly enhanced. This also predicts that the actin membrane

skeleton is more concentrated near the stimulation point and becomes more sparse than that before stimulation in the area far from the stimulation point.

#### Actin is Also Concentrated at and near the Stimulation Point

The actin distribution after point stimulation was examined by TIRF microscopy of the actin-GFP expressed in Jurkat cells (Figure 5). Actin was concentrated at and around the stimulation



**Figure 5.** Concentration of actin filaments at and near the stimulation point, as observed by actin-GFP. The contours of the stimulation points are shown in magenta lines. After mild treatments with 4 mM M $\beta$ CD or 10  $\mu\text{M}$  cytochalasin D for 15 min, the assembly of actin-GFP was blocked. Bar: 3  $\mu\text{m}$ .

point. After mild treatments with M $\beta$ CD or cytochalasin D, the assembly of actin-GFP was blocked. The effect of cytochalasin D suggests that filamentous actin, rather than G-actin, is responsible for such actin assembly. The effect of M $\beta$ CD on the assembly of actin-GFP indicates the possibility that, as explained at the end of the "Assembly of Lck- and N10-GFP at the Site of TCR Clustering (Stimulation Point)" subsection, Lck recruitment and actin concentration proceed hand in hand by concurrently enhancing each other. Meanwhile, the possibility exists that the loss of rafts is due to the M $\beta$ CD effect of dispersing PIP2 clusters by raft disruption, which are one of the major actin binding sites.

#### Bulk Stimulation of TCR Decreases the Diffusion Rates of Lck- and N10-GFP Everywhere in the Cell Membrane

Instead of local stimulation, the Jurkat cells were stimulated in the bulk solution by an incubation with the anti-CD3 antibody, OKT3. The  $D_{100\text{ ms}}$  values for both Lck- and N10-GFP were decreased after the bulk stimulation of the Jurkat cells, as shown

in the histograms in Figure 6. Since these clusters are dispersed throughout the cell surface, this result is consistent with the local stimulation results.

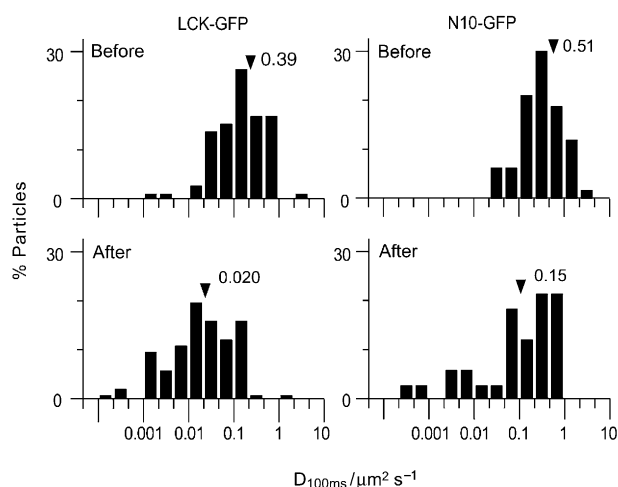


**Figure 6.** The  $D_{100\text{ ms}}$  values for Lck- and N10-GFP were decreased after the bulk stimulation of Jurkat cells. Anti-CD3 antibody was added to the Jurkat cells (in which the movements of Lck- and N10-GFP were observed) on the microscope stage, and the movements of individual Lck and N10 molecules were observed by TIRF microscopy after a 5 min incubation. The numbers indicate the median values.

### The Model for Lck Assembly at the TCR Cluster

The most critical points in the present investigation are the development of a local stimulation strategy and the single molecule observations of Lck- and N10-GFP. With our new data, based on these approaches, we propose a new model for Lck recruitment and concentration at and around the stimulation point (Figure 7). First, when the signal is triggered by TCR

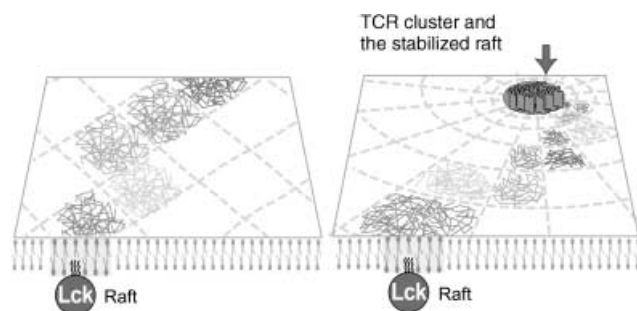


**Figure 7.** A model for Lck assembly at the TCR stimulation point. TCR clustering induces actin reorganization, causing the concentration of actin filaments around the TCR cluster, and thus forming a denser actin membrane skeleton at and near the stimulation point. In areas far from the stimulation point, the actin membrane skeleton may become sparse. Since the Lck- and N10-GFP molecules that are on the rafts may be strongly corralled by the actin membrane skeleton fence, as well as by the transmembrane picket proteins anchored to the membrane skeleton, the diffusion of Lck- and N10-GFP is substantially slowed and their binding to and interaction with the TCR cluster and the downstream signaling molecules are enhanced. Lck partitioning into the TCR-cluster stabilized raft and/or coalescence of Lck rafts with the TCR-cluster raft may induce higher concentrations of Lck on and near the stimulation point.

clustering, actin reorganization is induced. Initially, this may occur due to either the binding of actin filaments to the TCR cluster  $\zeta$  chains or the induction of the initial signal by a small number of Lck molecules, which are recruited by diffusional collision and subsequently entrapped by the TCR cluster. This might cause the actin filaments to become concentrated around the TCR cluster, thus forming a denser actin membrane skeleton, as shown in this work (see Figure 5). Dustin and Cooper<sup>[23]</sup> and Wülfing and Davis<sup>[24]</sup> also showed a similar assembly of actin filaments at this early stage. Due to this augmentation of the actin skeleton near the stimulation point, in areas far from the stimulation point, the actin membrane skeleton may become sparse. Since Lck- and N10-GFP and the rafts they associate with may be corralled by the actin membrane skeleton fence, as well as by the transmembrane picket proteins anchored to the membrane skeleton,<sup>[17, 22]</sup> an increase in the actin membrane skeleton meshwork density near the stimulation point will result in the slower diffusion of the Lck- and N10-GFP molecules and the rafts with which they are associated.

The reduced diffusion coefficient near the stimulation point would increase the residency time of Lck around the TCR cluster, and since compartmentalization does not decrease the rotational diffusion rate of Lck (rotational reorientation is necessary, in addition to bimolecular collision, which depends on translational diffusion, for the bimolecular binding and reactions, because the two molecules must have the correct orientations for the molecular interactions to occur), the chances for the Lck molecules to bind to the TCR cluster and the downstream effector molecules should increase near the TCR cluster region. Such interactions would augment the signaling for actin reorganization via the SLP-76 pathway,<sup>[25]</sup> which would in turn enhance the further assembly of Lck and other signaling molecules at and near the TCR cluster and their binding to the cluster and other signaling molecules.

How might the raft, which appears to be required for the Lck assembly, be involved in such concentration processes? Since we have not detected directed movements of Lck, we do not think that Lck is carried with the raft by the actomyosin motor system. However, the possibility still exists that Lck is transiently (less than the duration of several video frames, that is, less than 100 ms) associated with the raft traveling to the stimulation point. Although the Lck association with such a raft is transient, if there are many rafts being transported toward the stimulation point, then Lck as a whole would be concentrated toward the stimulation point. A more likely possibility is that the raft may be temporarily trapped in or bound to the membrane skeleton mesh of the actin filaments. In either case, the augmented (reduced) density of the actin membrane skeleton near (in the area far from) the stimulation point would reduce (increase) the diffusion coefficient. This would be true even for the Lck and N10 molecules located outside the rafts, but these effects would be greatly enhanced if these molecules were localized in the raft, because the rafts or the molecular complexes associated with the rafts would be much more susceptible to small changes in the density of the actin filaments than monomeric Lck or N10 molecules. In this sense, the association of Lck with a raft is needed to enhance the corraling and tethering effects of the

actin membrane skeleton mesh. In addition, the raft may keep the Lck concentrations high at and near the TCR cluster. Lck may partition into the TCR-cluster raft and/or the rafts with Lck may coalesce with those containing the TCR cluster, which would raise the Lck concentration in the neighborhood of the TCR cluster. These possibilities are now under investigation in our laboratories.

*We would like to thank G. Marriott for providing the cDNA for actin-GFP and Junko Kondo for the artwork.*

- [1] L. P. Kane, J. Lin, A. Weiss, *Curr. Opin. Immunol.* **2000**, *12*, 242–249.  
 [2] W. Zhang, L. E. Samelson, *Semin. Immunol.* **2000**, *12*, 35–41.  
 [3] G. Iezzi, K. Karjalainen, A. Lanzavecchia, *Immunity* **1998**, *8*, 89–95.  
 [4] G. J. Kersh, E. N. Kersh, D. H. Fremont, P. M. Allen, *Immunity* **1998**, *9*, 817–826.  
 [5] C. Pioli, L. Gatta, D. Frasca, G. Doria, *European J. Immunol.* **1999**, *29*, 856–863.  
 [6] B. A. Freiberg, H. Kupfer, W. Maslanik, J. Delli, J. Kappler, D. M. Zaller, A. Kupfer, *Nat. Immunol.* **2002**, *3*, 911–917.  
 [7] C. R. Monks, B. A. Freiberg, H. Kupfer, N. Sciaky, A. Kupfer, *Nature* **1998**, *395*, 82–86.  
 [8] R. Iino, I. Koyama, A. Kusumi, *Biophys. J.* **2001**, *80*, 2667–2677.  
 [9] R. Iino, A. Kusumi, *J. Fluores.* **2001**, *11*, 187–195.  
 [10] P. S. Kabouridis, J. Janzen, A. L. Magee, S. C. Ley, *Eur. J. Immunol.* **2000**, *30*, 954–963.  
 [11] A. S. Shaw, K. E. Amrein, C. Hammond, D. F. Stern, B. M. Sefton, J. K. Rose, *Cell* **1989**, *59*, 627–636.  
 [12] M. Moran, M. C. Miceli, *Immunity* **1998**, *9*, 787–796.  
 [13] S. C. Bunnell, V. Kapoor, R. P. Tribble, W. Zhang, L. E. Samelson, *Immunity* **2001**, *14*, 315–329.  
 [14] K. Yasuda, A. Kosugi, F. Hayashi, S. Saitoh, M. Nagafuku, Y. Mori, M. Ogata, T. Hamaoka, *J. Immunol.* **2000**, *165*, 3226–3231.  
 [15] A. Kosugi, J. Sakakura, K. Yasuda, M. Ogata, T. Hamaoka, *Immunity* **2001**, *14*, 669–680.  
 [16] A. Choidas, A. Jungbluth, A. Sechi, J. Murphy, A. Ullrich, G. Marriott, *Eur. J. Cell Biol.* **1998**, *77*, 81–90.  
 [17] T. Fujiwara, K. Ritchie, H. Murakoshi, K. Jacobson, A. Kusumi, *J. Cell Biol.* **2002**, *157*, 1071–1081.  
 [18] A. Kusumi, Y. Sako, M. Yamamoto, *Biophys. J.* **1993**, *65*, 2021–2040.  
 [19] Y. Sako, A. Nagafuchi, S. Tsukita, M. Takeichi, A. Kusumi, *J. Cell Biol.* **1998**, *140*, 1227–1240.  
 [20] J. R. Chan, S. J. Hyduk, M. I. Cybulsky, *J. Immunol.* **2000**, *164*, 746–753.  
 [21] S. Caplan, M. Baniyash, *Immunol. Today* **2000**, *1*, 223–228.  
 [22] A. Kusumi, Y. Sako, *Curr. Opin. Cell Biol.* **1996**, *8*, 566–574.  
 [23] M. L. Dustin, J. A. Cooper, *Nat. Immunol.* **2000**, *1*, 23–29.  
 [24] C. Wülfing, M. M. Davis, *Science* **1998**, *282*, 2266–2269.  
 [25] J. Bubeck Wardenburg, R. Pappu, J. Y. Bu, B. Mayer, J. Chernoff, D. Straus, A. C. Chan, *Immunity* **1998**, *9*, 607–616.

Received: February 26, 2003 [Z670]

## Bis( $\mu$ -oxo)dicopper as Key Intermediate in the Catalytic Decomposition of Nitric Oxide

Marijke H. Groothaert,<sup>[a]</sup> Kristof Lievens,<sup>[a]</sup> Jeroen A. van Bokhoven,<sup>[b]</sup> Andrea A. Battiston,<sup>[b]</sup> Bert M. Weckhuysen,<sup>[b]</sup> Kristine Pierloot,<sup>[c]</sup> and Robert A. Schoonheydt<sup>\*[a]</sup>

### KEYWORDS:

copper · heterogeneous catalysis · UV/Vis spectroscopy · O ligands · zeolites


The direct decomposition of NO into N<sub>2</sub> and O<sub>2</sub> is the simplest and most desirable approach to NO abatement. Although no catalysts are known that fulfill all criteria required for application, some materials show a high NO conversion and could be potential catalysts in the near future.<sup>[1, 2]</sup> The copper-loaded ZSM-5 zeolite is the most studied catalyst with a high and stable NO decomposition activity. Since its discovery in 1986,<sup>[3]</sup> considerable research efforts have been made in order to unravel the reaction mechanism and the active sites in Cu-ZSM-5.<sup>[1–8]</sup> A growing consensus is found that a redox process cycling between Cu<sup>+</sup> ions and Cu<sup>2+</sup>-ELO species is present (ELO = extra lattice oxygen).<sup>[1, 4–6]</sup> However, the nature of the Cu<sup>2+</sup>-ELO species has so far not unequivocally been identified.<sup>[1, 4–7]</sup>

Here, we report on the elucidation of this catalysis by identifying the bis( $\mu$ -oxo)dicopper species as the key intermediate that allows the smooth formation and desorption of O<sub>2</sub>. The detection of the bis( $\mu$ -oxo)dicopper species and its role was made possible by in situ spectroscopy, that is, under real reaction conditions. Firstly, UV/Vis monitoring of the catalyst using optical fiber technology was combined with on-line GC analysis.<sup>[9]</sup> Secondly, direct structural information of the catalyst under working conditions was obtained with XAS (X-ray absorption spectroscopy).<sup>[10, 11]</sup> So far, the bis( $\mu$ -oxo)dicopper core had only been characterized in homogeneous, synthetic complexes.<sup>[12]</sup> Its isomerized ( $\mu$ - $\eta^2$ : $\eta^2$ -peroxo)dicopper core is present in natural

[a] Prof. R. A. Schoonheydt, Dr. M. H. Groothaert, K. Lievens  
 Center for Surface Chemistry and Catalysis  
 Katholieke Universiteit Leuven  
 Kasteelpark Arenberg 23, 3001 Leuven (Belgium)  
 Fax: (+32) 16-321-998  
 E-mail: robert.schoonheydt@agr.kuleuven.ac.be

[b] Dr. J. A. van Bokhoven, Dr. A. A. Battiston, Prof. B. M. Weckhuysen  
 Department of Inorganic Chemistry and Catalysis  
 Debye Institute, Utrecht University  
 Sorbonnelaan 16, 3584 CA Utrecht (The Netherlands)

[c] Prof. K. Pierloot  
 Department of Chemistry  
 Katholieke Universiteit Leuven  
 Celestijnenlaan 200F, 3001 Leuven (Belgium)

 Supporting information for this article is available on the WWW under <http://www.chemphyschem.org> or from the author.